EUROPHYSICS LETTERS 20 December 1994

Europhys. Lett., 28 (9), pp. 665-670 (1994)

Crystallization in Sedimentation Profiles of Hard Spheres.

T. BIBEN (*), R. OHNESORGE (**) and H. LÖWEN (**)

(*) *Laboratoire de Physique, Ecole Normale Supérieure de Lyon (URA CNRS 1325)*
46 Allée d'Italie - F-69364 Lyon Cedex 07, France
(**) *Sektion Physik der Universität München*
Theresienstraße 37, D-80333 München, Germany

(received 2 September 1994; accepted in final form 8 November 1994)

PACS. 68.45 – Solid-fluid interface processes.
PACS. 82.70D – Colloids.
PACS. 61.20 – Classical, semiclassical, and quantum theories of liquid structure.

Abstract. – Equilibrium density profiles of a hard-sphere suspension in a gravitational field are calculated using Monte Carlo simulations. For increasing gravity there is a *discontinuous* freezing transition induced by the container wall where few crystalline layers are spontaneously formed at the bottom of the sample. This crystalline part then grows *continuously* as the gravitational field is further enhanced. The results are compared with density functional theory of freezing where a weighted density approximation is used. While good overall agreement of the laterally averaged profile and the lateral crystallinity is achieved, density functional theory yields a discontinuous crystal growth via layering transitions.

Equilibrium sedimentation profiles of colloidal suspensions in a gravitational field have stimulated statistical mechanics of inhomogeneous fluids since 1910 when Perrin estimated Avogadro's constant directly from measurements of profiles of dilute suspensions. By now the density profile of well-characterized charged or sterically stabilized suspensions can be accurately measured using depolarized light scattering [1]. By inverting the density profile of a weakly inhomogeneous fluid one can determine the isothermal osmotic equation of state directly [2,3]. Also the sedimentation dynamics [4] can be resolved on an experimentally accessible time scale [5] through visualization of the sedimentation and crystallization mechanism.

While most of the recent calculations assume a weak modulation of the fluid phase by the external field, we focus on *microscopic* (or better mesoscopic) aspects of the density profile including crystallization effects. The motivation in doing so is threefold:

1) The influence of the bottom of the sample on the microscopic density field has not yet been examined in detail. For increasing gravitational-field strength, the fluid system undergoes a freezing transition forming crystalline layers at the bottom of the sample. Details of this wall-induced crystallization transition, however, are not clear at the moment. With few crystalline layers at the bottom the strongly inhomogeneous profile also consists of a crystal-fluid interface and a low-density tail. If the strength of the gravitational field is increased further while keeping the total particle density fixed, the crystalline portion will

grow at the expense of the fluid part. The *nature of crystal growth* is *a priori* not clear. In particular, crystal growth may be continuous or proceed via a series of first-order surface phase transitions corresponding to layering. This can only be answered from a microscopic calculation.

2) Taking the availability of simulation data for granted, a system with coexisting crystal and fluid phases in a strong external field is an ideal *test* system for the validity of density functional theory of freezing.

3) In experiments on colloidal suspensions, one can resolve the density field on the length scale of a typical interparticle spacing [6] using real-space methods (*e.g.*, direct image processing or microscopy). The strength of the gravity can be controlled by adding a solvent with a different density. Thus an *experimental* verification of theoretical predictions concerning the crystallization mechanism in a strong external field is possible.

In this letter we study the hard-sphere system in a strong gravitational field which is directed along the z-axis and can be written as the external potential

$$V(z) = \begin{cases} mgz\,, & \text{if } z \geqslant 0\,, \\ \infty\,, & \text{if } z < 0\,, \end{cases} \tag{1}$$

where m is the buoyant mass of the colloidal particles and g the gravitational acceleration. The strength of the interaction is conveniently measured by the dimensionless ratio $\alpha = mg\sigma/k_B T$, σ denoting the hard-sphere diameter and T the temperature. The only additional thermodynamic parameter then is the mean area density $\bar{\rho}$ defined as the number of particles per unit area of the bottom of the sample. The bulk hard-sphere system exhibits stable fluid and dense-packed crystalline phases. For strong gravity, the crystalline phase appears at the bottom of the sample.

Monte Carlo simulations are used to compute the one-particle density field $\rho(\boldsymbol{r})$ of the spheres. Particular emphasis is placed on the laterally averaged density exhibiting sharp peaks in the solid phase and on the lateral crystalline structure. Based on these two target quantities, the following scenario of crystallization is obtained for increasing α and fixed $\bar{\rho}$: first there is a wall-induced discontinuous freezing transition where few crystalline layers are spontaneously formed at the bottom. This crystalline portion then grows continuously at the expense of the fluid part of the profile. Similar simulations were recently done for zero gravity ($\alpha = 0$) resulting in precrystallization of the hard-sphere fluid near a hard wall [7]. However, the onset of crystallization and the subsequent growth for increasing bulk pressure was not yet studied in detail.

The Monte Carlo simulations are performed in a similar way as in ref. [3]. $N = 500$ particles are confined to a slab which is infinite in the z-direction and rectangular in the x and y directions. Periodic boundary conditions are used in the x and y directions. The starting configuration consists of two crystalline layers at the bottom and a disordered part for higher z. About 10^5 Monte Carlo moves per particle have been used to equilibrate the system and again $2 \cdot 10^5$ moves to gather statistics for the density field. The centre-of-mass motion in the x and y directions was fixed in order to avoid a spurious diffusion of the whole finite-sized lattice.

The laterally integrated density profile is defined as

$$\rho^{\perp}(z) = \frac{1}{A} \int \mathrm{d}x \int \mathrm{d}y\, \rho(x, y, z)\,, \tag{2}$$

where A is the area of the bottom. Monte Carlo results for $\rho^{\perp}(z)$ are shown in fig. 1 for different values of α ranging from 2.0 to 4.5 and fixed $\bar{\rho}\sigma^2 = 5.43$. For $\alpha \leqslant 2.5$, the interstitial density is high indicating that the system is a strongly perturbed liquid. For $\alpha \simeq 2.75$ this density drops discontinuously to very small values in the first two layers, indicating that the first two layers are crystalline. Also the peak position of the third and fourth layer changes practically in a discontinuous manner between $\alpha = 2.5$ and $\alpha = 2.75$ although these peaks remain fluid-like. As α is enhanced further ($\alpha > 2.75$) these peaks become gradually crystal-like, but the crystal growth is continuous as a function of α.

The same scenario can be seen in the lateral crystalline order which is measured by introducing the order parameter

$$c(z) = \frac{\int \mathrm{d}x \int \mathrm{d}y\, \mathcal{G}(x, y)\rho(x, y, z)}{\int \mathrm{d}x \int \mathrm{d}y\, \rho(x, y, z)}, \tag{3}$$

where the kernel $\mathcal{G}(x, y)$ probes any triangular order in the layer

$$\mathcal{G}(x, y) = \frac{4}{3}\cos\left(\frac{2\pi x}{a}\right)\cos\left(\frac{\pi}{a}(x + \sqrt{3}y)\right)\cos\left(\frac{\pi}{a}(x - \sqrt{3}y)\right) - \frac{1}{3}. \tag{4}$$

Here a is the nearest-neighbour distance of the triangular lattice and the lattice is oriented such that one lattice vector is in the x-direction. In the definition of $c(z)$, only second- and higher-order stars of the reciprocal triangular lattice are involved. Consequently only

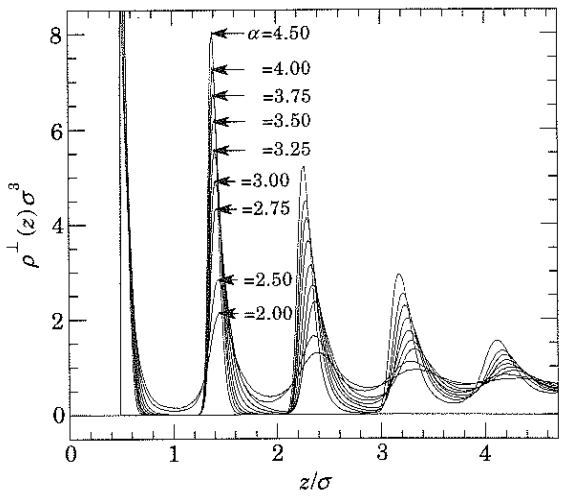

Fig. 1.

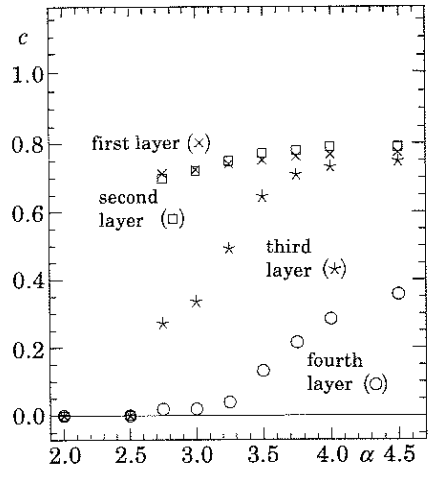

Fig. 2.

Fig. 1. – Nine laterally integrated density profiles $\rho^{\perp}(z)\sigma^3$ obtained from computer simulation for $\alpha = 2.0$, 2.5, 2.75, 3.0, 3.25, 3.5, 3.75, 4.0, 4.5 and fixed average density $\bar{\rho} = 5.43$.

Fig. 2. – Maximum of the crystallinity $c(z)$ in the first four layers as a function of α ($\bar{\rho} = 5.43$) as obtained from computer simulation: first layer (crosses), second layer (squares), third layer (stars), fourth layer (circles).

density variations which have a joint spatial variation in both triangular directions are probed by $c(z)$. For a laterally homogeneous density and for simple plane waves, $c(z)$ vanishes. Monte Carlo results for $c(z)$ are displayed in fig. 2 as a function of α, where z is taken to correspond to the peak position of the first four layers. Again one sees the discontinuous behaviour in c at $\alpha \equiv \alpha_c \approx 2.6$ for the first three layers, implying spontaneous formation of two-dimensional long-range crystalline order. For higher α there is a smooth variation of c in α. This indicates that once the wall freezing has set in, there are no further first-order surface phase transitions nor discontinuous layering transitions. The question of layering was also discussed in the context of surface melting [8] of, *e.g.*, Lennard-Jones systems [9, 10] where it was tentatively found to occur. This is, however, a different situation since there are two interfaces (solid–quasi-liquid and quasi-liquid–gas) whose interaction may cause layering. In our case there is only the fixed bottom wall and the crystal-liquid interface which continuously moves as α is enhanced.

We also present density functional calculations of the hard-sphere sedimentation profiles. In particular we adopt the weighted-density approximation (WDA) introduced by Curtin and Ashcroft some years ago [11], which leads to one of the best freezing theories to date. The minimization of the WDA functional was performed practically freely on a fine equidistant grid with $\mathcal{N} = 10^6$ grid points in a slab compatible with lateral periodicity of a (111) direction of an f.c.c. crystal (for details see ref. [10]). In the z-direction the total system size was 18σ with periodic boundary conditions, which is large enough to prevent spurious interaction of the periodically repeated bottom with the solid-fluid interface. The minimization was performed—under the constraint of fixed averaged area density $\bar{\rho}$—also with respect to the size of the slab. The high number of grid points is sufficient to resolve the rapid spatial density variations in the solid phase.

In fig. 3*a*) computer simulation data (solid line) and density functional data (dashed line) for $\rho^{\perp}(z)$ are compared, where the parameters are $\alpha = 3$ and $\bar{\rho}\sigma^2 = 5.43$. Both profiles show sharp peaks at the bottom corresponding to 2-3 crystalline layers, a crystal-fluid interface and a dilute tail for $z \to \infty$. The contact value of $\rho^{\perp}(z)$ at the bottom ($z = \sigma/2$) is fixed by the

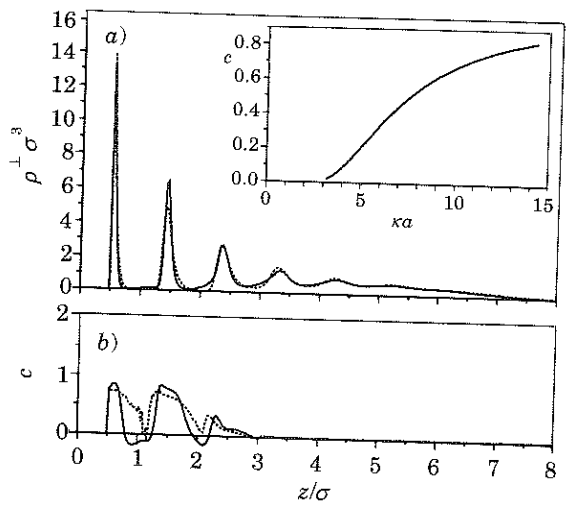

Fig. 3. – *a*) Laterally integrated density profile $\rho^{\perp}(z)\sigma^3$ *vs.* z/σ for hard spheres in a gravitational field ($\alpha = 3$, $\bar{\rho} = 5.43$): Monte Carlo results (broken line) and density functional theory (solid line). The inset shows the z-independent value of c for a set of normalized Gaussian peaks $\propto \exp[-\kappa^2 r^2]$ on an f.c.c. lattice *vs.* κa. *b*) Lateral crystallinity $c(z)$ *vs.* z/σ: density functional theory (solid line) and simulation results (broken line).

wall theorem $\rho^{\perp}(z = \sigma/2) = P/k_B T$, where P is the pressure at the bottom. The WDA satisfies this relation. Therefore the two profiles exactly coincide at $z = \sigma/2$. Also the results for the dilute tail nearly coincide. In the intermediate range the height of the peaks is higher in density functional theory than in the simulation. This can be simply attributed to the fact that the WDA [11, 10] underestimates the solid coexisting density and overestimates the sharpness of the solid peaks [12]. The overall agreement of the sedimentation profiles is still quite satisfactory. Also the results for the nearest-neighbour distance a of the triangular lateral lattice are very close: in density functional theory a was determined by free minimization to be 1.153σ, whereas the simulation result is $a = 1.088\sigma$. In the simulation different runs with different lateral box sizes were performed and the correct a was obtained by requiring consistency of the bottom pressure $P = mg\bar{\rho}$ with the wall theorem $P = k_B T \rho^{\perp}(\sigma/2)$.

Full z-dependent lateral crystallinities as defined by (3) are compared in fig. 3*b*). If $\rho(\boldsymbol{r})$ consisted of a superposition of strongly peaked Gaussians, $c(z)$ would be independent of z. In the inset of fig. 3, we have shown how c depends then on the sharpness of the Gaussian peaks. For infinitely sharp δ-peaks c is normalized to be 1. The Monte Carlo data for $c(z)$ agree fairly well with the WDA results near the peak maxima. Also the strong peak asymmetry (*i.e.* the shift of the position of the maximum towards smaller z-values with respect to its layer average) is qualitatively similar in density functional theory and simulation. Furthermore density functional theory yields an oscillatory behaviour which is even negative in the interstitial region. Whether this is a real feature or an artifact of the density functional theory due to the wrong anisotropy of the density in the solid phase [12] remains somewhat unclear at the moment. The Monte Carlo data are also inconclusive in the interstitial region, since it is a very rare event that a particle position falls between two crystalline layers, which causes a large statistical error. The value of $c = 0.8$ corresponds roughly to a localization length of $1/\kappa = 0.1\sigma$ of the Gaussian peaks $\simeq \exp[-\kappa^2 r^2]$. While the WDA is capable of describing such strongly inhomogeneous sedimentation profiles qualitatively and quantitatively correctly, details of the crystal growth are not reproduced exactly. Free minimization of the WDA functional yields a discontinuous crystal growth via a series of layering transitions as α is enhanced [13]. This failure can be understood simply by the fact that density functional theory is a mean-field theory neglecting any capillary-wave–like fluctuations of the crystal-fluid interface which smear out a discontinuity [8].

To summarize, we have presented evidence that crystallization of hard spheres in a strong gravitational field starts discontinuously and proceeds continuously and not by layering transitions. This should at least in principle be detectable experimentally in real sedimentation profiles of sterically stabilized index-matched colloidal suspensions. Moreover, a comparison of the WDA density functional theory and Monte Carlo results for the density distribution of the strongly inhomogeneous hard-sphere system in a gravitational field was performed. The overall agreement was satisfactory, indicating that the WDA is capable of describing inhomogeneous crystal-fluid interfaces well within the limitations of a slightly shifted bulk phase diagram. However, density functional theory fails in describing a continuous crystal growth.

We conclude with two final remarks: first, we note that the density functional approach of freezing can also be transferred to binary hard-sphere mixtures [14]. In this case already the limit of weak fluid density variations exhibits an interesting non-monotonic density field for the two kinds of spheres [15]. Including also crystalline phases, this behaviour might be expected to be even richer and more complex. Secondly, there is no computer simulation for the surface tension of a free crystal-fluid interface. Such a simulation is highly desirable in order to check the density functional predictions for the hard-sphere surface tensions [10].

* * *

We thank J. P. HANSEN for useful comments on the manuscript. This work was supported by the French-German PROCOPE exchange program under contract No. 312-pro-93-as and by the Bundesministerium für Forschung und Technologie (BMFT) under contract No. 03WA2LMU.

REFERENCES

[1] PIAZZA R., BELLINI T. and DEGIORGIO V., *Phys. Rev. Lett.*, **71** (1993) 4267.
[2] BARRAT J. L., BIBEN T. and HANSEN J. P., *J. Phys. Condens. Matter*, 4 (1992) L11.
[3] BIBEN T., HANSEN J. P. and BARRAT J. L., *J. Chem. Phys.*, **98** (1993) 7330.
[4] MILLS P. and SNABRE P., *Europhys. Lett.*, **25** (1994) 651.
[5] VAN DUIJNEVELDT J. S., DHONT J. K. G. and LEKKERKERKER H. N. W., *J. Chem. Phys.*, **99** (1993) 6941.
[6] VONDERMAßEN K., BONGERS J., MUELLER A. and VERSMOLD H., *Langmuir*, **10** (1994) 1351.
[7] COURTEMANCHE D. J. and VAN SWOL F., *Phys. Rev. Lett.*, **69** (1992) 2078; COURTEMANCHE D. J., PASMORE T. A. and VAN SWOL F., *Mol. Phys.*, **80** (1993) 861.
[8] For a review see: LÖWEN H., *Phys. Rep.*, **237** (1994) 249.
[9] VALKEALATHI S. and NIEMINEN R. M., *Phys. Scr.*, **36** (1987) 646.
[10] LÖWEN H., OHNESORGE R. and WAGNER H., *Ber. Bunsenges. Phys. Chem.*, **98** (1994) 303; OHNESORGE R., LÖWEN H. and WAGNER H., to be published in *Phys. Rev. E*.
[11] CURTIN W. G. and ASHCROFT N. W., *Phys. Rev. A*, **32** (1985) 2909.
[12] OHNESORGE R., LÖWEN H. and WAGNER H., *Europhys. Lett.*, **22** (1993) 245.
[13] For further details see: OHNESORGE R., Ph.D. Thesis, University of Munich (1994).
[14] BARRAT J. L., BAUS M. and HANSEN J. P., *Phys. Rev. Lett.*, **56** (1986) 1063; *J. Phys. C*, **20** (1987) 1413.
[15] BIBEN T. and HANSEN J. P., *Mol. Phys.*, **80** (1993) 853.